Advanced Hysteresis Control of Brushless DC Motors

Joachim Böcker
University of Paderborn, Germany
Institute of Power Electronics and Electrical Drives
boecker@lea.upb.de

***Abstract*—Brushless DC motor drives are typically employed in speed controlled applications. Torque control, particularly during regenerative mode, is not the standard domain of BLDC drives. However, it can be shown that the known BLDC control approach can be extended to control the torque in the regenerative mode even for low speed or at standstill. A hysteresis controller is proposed, which is specified by means of a state chart.**

I. Introduction

A brushless DC motor drive usually consists of a voltage source inverter and a three-phase permanent magnet motor quite similar to a standard three-phase drive (Fig. 1). However, the BLDC operation mode, using only two of three active phases at a time, enables a quite simple control approach compared, e.g., with the flux-oriented control of a three-phase permanent magnet motor. BLDC drives are mostly used for speed-controlled applications in driving operation. The torque-controlled operation, particularly in the regenerative mode, is not the usual domain of BLDC drives. This paper, however, shows how to revise the standard BLDC control approach to enable even regenerative operation.

II. Conventional BLDC Control

The typical BLDC operation mode is that, depending on the rotor position, one of the three inverter legs is kept inactive so that the current of that phase is then usually zero. There exists only one current path through both of the active inverter legs and the corresponding motor phases. One of the active inverter legs serves as buck converter in order to regulate the current, while the second active leg connects the motor to the positive or the negative DC link potential.

The control objective is mostly the speed. A speed controller may directly determine the duty cycle of a pulse width modulator (PWM), Fig. 2, or a cascaded control with an outer speed and an inner current control loop may be employed. The inner current control may be a PI-type controller with pulse width modulator as shown in Fig. 3, or a hysteresis controller, Fig. 4. This paper, however, will focus on the current control loop of the latter structure.

The motor phase currents resulting from that kind of control will show the typical square wave shapes. If a special BLDC motor with trapezoidal EMF is employed, the resulting torque is constant and proportional to the amplitude of the currents. The BLDC approach, however, can also be applied to permanent magnet motors with sinusoidal EMF, but the torque will then include a 6th-order harmonic content.

The control approaches with inner current control loop differs in the way, how the current feedback I is generated. The simplest solution is to use the DC link current,

$$I = i_{dc} \tag{1}$$

That method, however, may cause problems at standstill and low speed, because the DC link current is very small

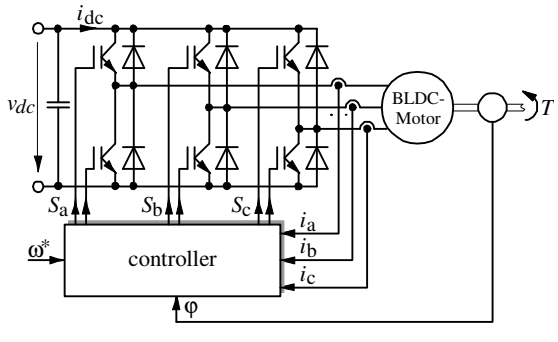

Fig. 1. BLDC drive

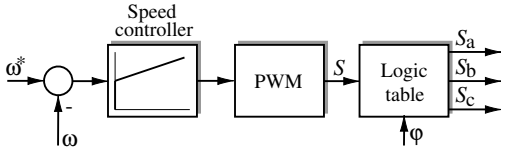

Fig. 2. Speed control with PWM

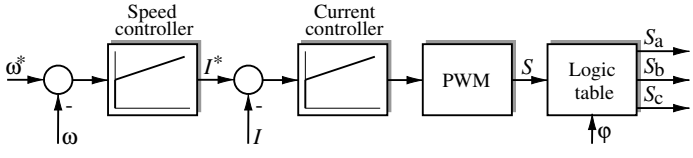

Fig. 3. Cascaded control with PWM

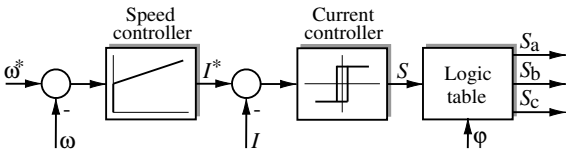

Fig. 4. Cascaded control with hysteresis current control

TABLE I
DETERMINATION OF THE CURRENT TO BE CONTROLLED

area	φ [1]	$2I$	V
1	-30°, 30 °	$i_b - i_c$	$v_b - v_c$
2	30°, 90°	$i_b - i_a$	$v_b - v_a$
3	90°, 150°	$i_c - i_a$	$v_c - v_a$
4	150°, 210°	$i_c - i_b$	$v_c - v_b$
5	210°, 270°	$i_a - i_b$	$v_a - v_b$
6	270°, 330°	$i_a - i_c$	$v_a - v_c$

[1] The angle $\varphi = 0$ is that position, the free motor will take with currents $i_a > 0, i_b = i_c = -i_a / 2$.

even with large motor currents. As alternative solution, e.g. [3], I can be generated from the motor phase currents by

$$I = \frac{1}{2} \sum_{k=a,b,c} |i_k| \quad \text{or} \quad I = \max_{k=a,b,c} \{|i_k|\} \qquad (2)$$

Because one of the phase currents should be zero, the sum yields the amplitude of the square wave. But this approach can handle only the driving operation. In view of governing also the regenerative mode, I should be better determined by selection of the appropriate phase current depending on the rotor position as proposed in Table I, where the correct signs of the phase currents are considered.

TABLE II
INVERTER SWITCHING COMMANDS FOR DRIVING OPERATION

area	φ	S_a	S_b	S_c
1	-30°, 30 °	0	+1	$-S$
2	30°, 90°	–1	S	0
3	90°, 150°	$-S$	0	+1
4	150°, 210°	0	–1	S
5	210°, 270°	+1	$-S$	0
6	270°, 330°	S	0	–1

The switching command S, either that of the PWM or of the hysteresis controller, can take only two values that are denoted as $S = \{+1,0\}$. Depending on the area of the rotor position, the command S is distributed to the inverter switching commands S_a, S_b, S_c by a logic table as specified by Table II. In that notation, "+1" or "–1" indicate that the upper transistor, or the lower one, respectively, is turned on. "0" indicates that both transistors are turned off. In this case, only the free wheeling diodes may conduct a current.

The result of this strategy is that the line-to-line voltage V between the active phases (see Table I for definition of

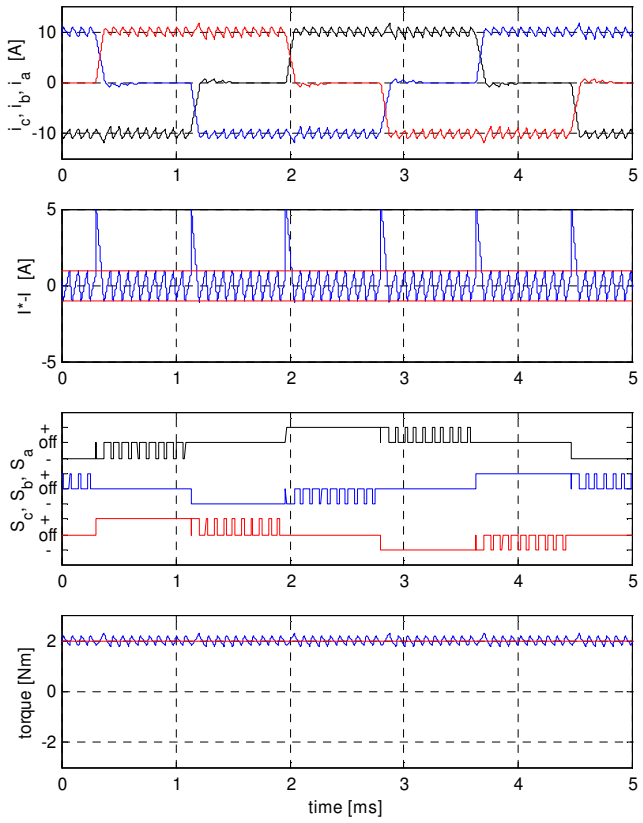

Fig. 5. Behavior in driving mode, $\omega / 2\pi$ =200 Hz

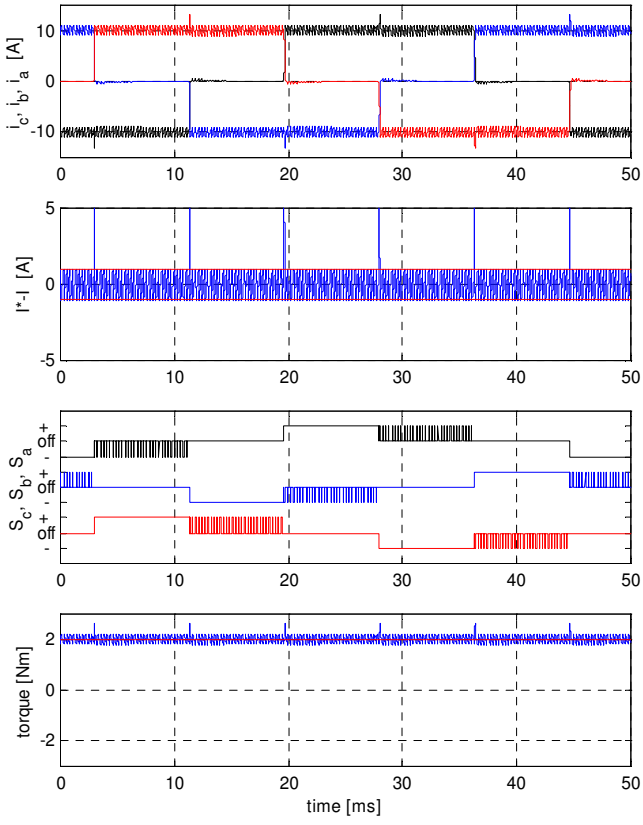

Fig. 6. Behavior in driving mode, $\omega / 2\pi$ =20 Hz

V) is always

$$V = Sv_{dc} = \{0,+1\}v_{dc} = \{0,+v_{dc}\} = \{V_0, V_+\} \quad . \tag{3}$$

Neglecting the commutation between the phases, the current behavior will follow the simple differential equation

$$\begin{aligned} 2L\dot{I} &= V - 2E - 2RI \\ &= \{V_0, V_+\} - 2\omega\psi_f - 2RI \end{aligned} \tag{4}$$

where E is the electromotoric force (EMF) of one phase, and R and L are the resistance and the inductance of one phase. As long as the sliding condition

$$V_0 = 0 < 2\omega\psi_f + 2RI^* < V_+ = v_{dc} \tag{5}$$

is ensured, the hysteresis controller will hold the current within the tolerance band. $V_+ = v_{dc}$ lets the current I increase, $V_0 = 0$ lets it decrease. The torque

$$T = 2n_p\psi_f I \tag{6}$$

is proportional to the current I , so torque control is equal to current control. The numbers of pole pairs is n_p

A typical behavior of the hysteresis current approach is shown in Fig. 5 and 6. The figures show the three phase currents i_a, i_b, i_c of the motor, the control error $I^* - I$ together with the hysteresis width, the three inverter switching command signals S_a, S_b, S_c, and the torque compared with the desired value at constant speed. Fig. 5 shows the behavior for high speed, Fig. 6 for low speed.

III. Regenerative Operation

The described approach is even capable of regenerative operation with slight modifications: If, in case of driving operation, a transistor need not have to be turned on, because the parallel diode is conducting, it is now necessary to switch it on. Vice versa, a transistor, which is conducting in the driving mode, need not have to be switched on for regenerative operation. The result is a modified Table III.

The resulting behavior of the regenerative mode is shown in Fig. 7, which is quite satisfactory. However, with decreasing speed, the control behavior degrades essentially (Fig. 8). The control is no longer able to force the current back into the tolerance band, because the sliding condition

TABLE III
Inverter Switching Commands for Regenerative Operation

area	φ	S_a	S_b	S_c
1	-30°, 30 °	0	0	$1-S$
2	30°, 90°	0	$S-1$	0
3	90°, 150°	$1-S$	0	0
4	150°, 210°	0	0	$S-1$
5	210°, 270°	0	$1-S$	0
6	270°, 330°	$S-1$	0	0

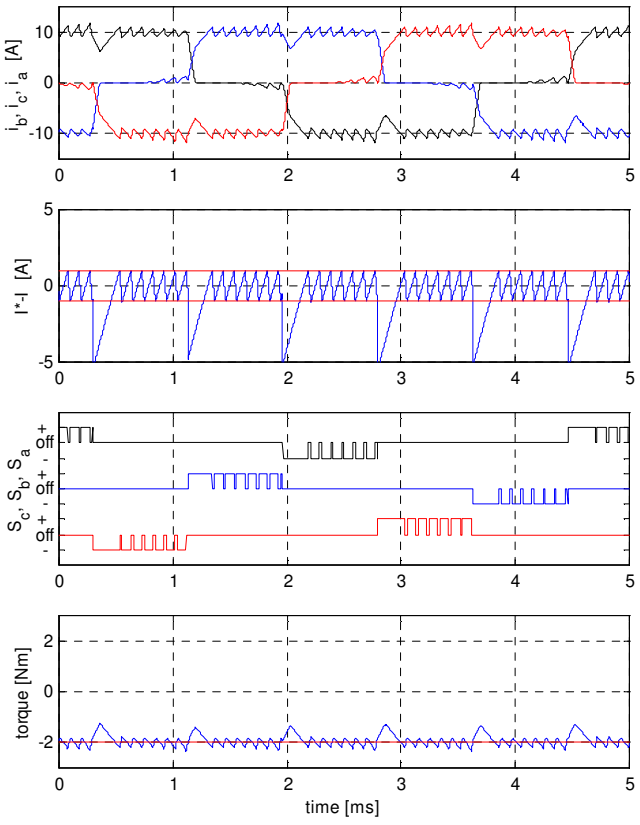

Fig. 7. Behavior in regenerative mode, $\omega/2\pi$ =200 Hz

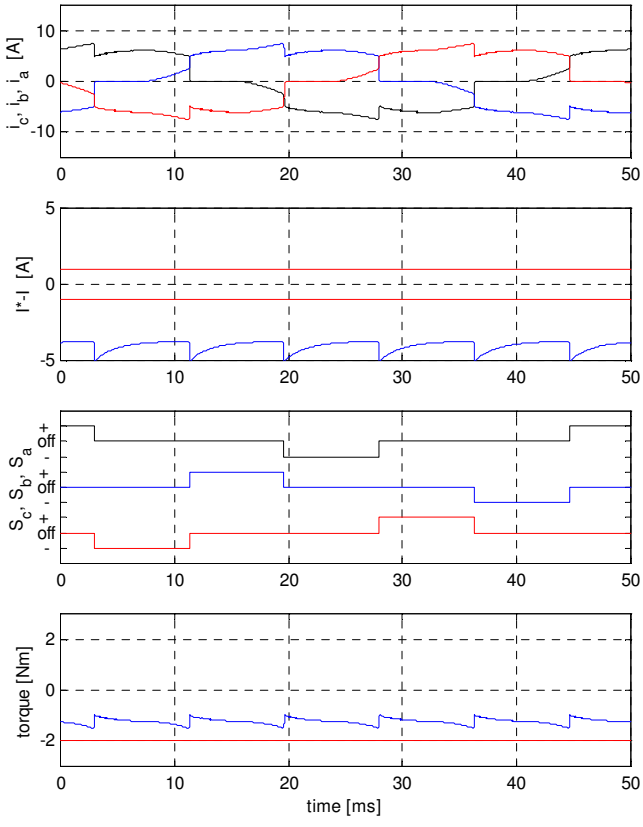

Fig. 8. Behavior in regenerative mode, $\omega/2\pi$ =20 Hz

(5) is violated. The minimum possible regenerative current can be calculated from (5) as

$$I > I_{\min} = -\frac{\omega \psi_f}{R} \quad . \tag{7}$$

IV. Improved Control Strategy

To overcome the problem of the regenerative mode and to exceed the limit (7), the controller should be allowed to use also the negative voltage $V = V_- = -v_{dc}$, which is possible by appropriate switching commands. The two active legs of the inverter work as four quadrant converter, which is able to apply positive and negative voltages as well. A difficulty is now that three switching states $V = \{-v_{dc}, 0, +v_{dc}\}$ have to be handled, which cannot be generated by a simple hysteresis controller with binary output S.

That is why the control concept was extended as shown in Fig. 9. The proposal incorporates now two tolerance bands $\pm\varepsilon_1$ and $\pm\varepsilon_2$. Usually, the controller works between the inner thresholds $\pm\varepsilon_1$ applying the voltages V_0 and V_+ alternatively. Only if the control error hits the second threshold $-\varepsilon_2$, the voltage V_- will be applied. As already shown for other converter topologies, [1], [2], state charts are an appropriate method to specify such control strategies pretty clear, which can be seen from Fig. 10. The state transitions are triggered by the events E_+, E_-, F_+, F_-, which

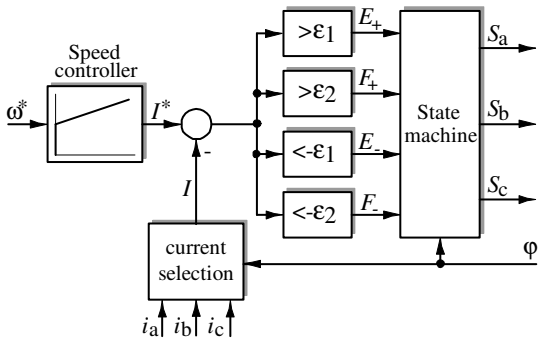

Fig. 9. Proposed control structure

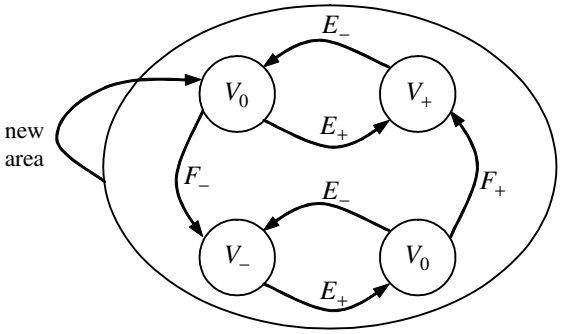

Fig. 10. State chart

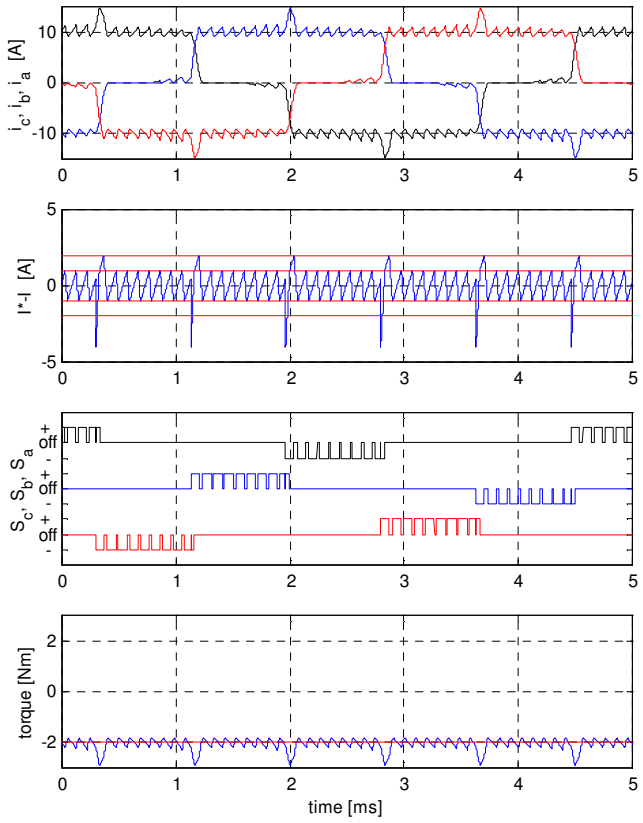

Fig. 11. Improved behavior in regenerative mode, $\omega/2\pi$ =200 Hz

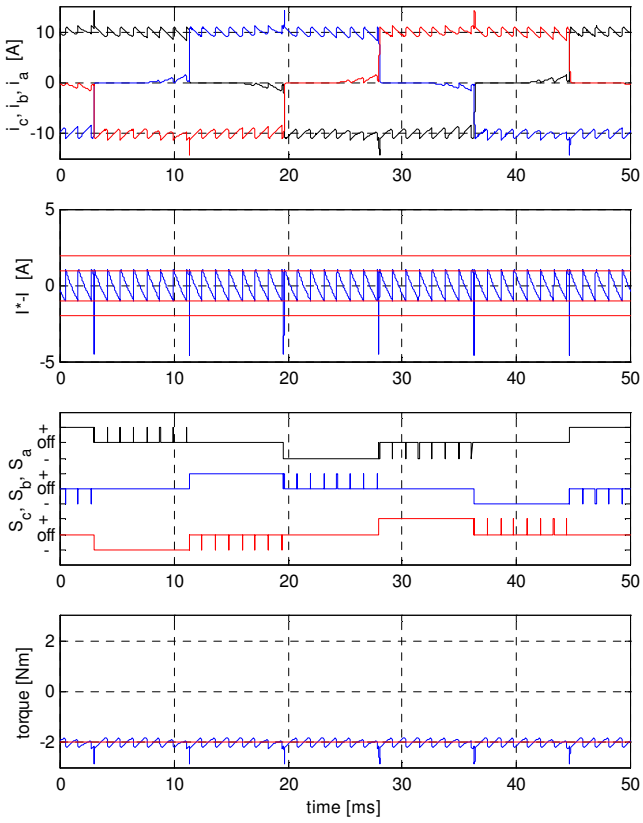

Fig. 12. Improved behavior in regenerative mode, $\omega/2\pi$ =20 Hz

TABLE IV
INVERTER SWITCHING COMMANDS FOR COMPLETE OPERATION RANGE

area	$I^* > 0$			$I^* < 0$		
	V_-	V_0	V_+	V_-	V_0	V_+
1	0, 0, 0	0,+1, 0	0,+1, –1	0,–1,+1	0, 0,+1	0, 0, 0
2	0, 0, 0	–1, 0, 0	–1,+1, 0	+1, –1, 0	0, –1, 0	0, 0, 0
3	0, 0, 0	0, 0,+1	–1, 0,+1	+1, 0, –1	+1, 0, 0	0, 0, 0
4	0, 0, 0	0, –1, 0	0, –1,+1	0,+1, –1	0, 0, –1	0, 0, 0
5	0, 0, 0	+1, 0, 0	+1, –1, 0	–1,+1, 0	0,+1, 0	0, 0, 0
6	0, 0, 0	0, 0, –1	+1, 0, –1	–1, 0,+1	–1, 0, 0	0, 0, 0

indicate, if a threshold is hit. Each time, a new area of the angle is entered, the state is reset to V_0.

The resulting states of the graph of Fig. 10 have to be mapped to the particular inverter switching commands S_a, S_b, S_c, which are given by Table IV. The resulting commands depend on the area and the mode of operation, driving or regenerative. The controller is completely specified by the structure (Fig. 9), the state chart (Fig. 10), and the mapping table (Table IV). As a proposal, most of that functions can be implemented using a field programmable logic gate array (FPGA).

The results with that new control strategy are shown in Fig. 11 and 12. The control error is now depicted with the thresholds $\pm\varepsilon_1$ and $\pm\varepsilon_2$. Particularly Fig. 12, which is the result for low speed, shows that the desired torque is now fully achieved (compare with Fig. 8). The states toggle only between V_0 and V_-, which is the case, if the ohmic voltage drop is larger than the EMF E.

Even Fig. 10 for higher speed shows a better result than Fig. 7 with the original strategy. The states toggle mainly between V_0 and V_+, which is not different to Fig. 7, but, during a commutation, the negative voltage V_- is now applied for a short time so that the control error is much faster back within the thresholds.

V. CONCLUSION

It has been shown how to extend the hysteresis control of BLDC drives for regenerative operation even at small speed and standstill. The control approach does not need any supplement of power electronics or sensors. As a particular point of interest, the controller has been specified by means of a state chart, which is an appropriate method for the design of switching controllers. The control may be realized using a microcontroller, or, as alternative, a field programmable gate array (FPGA).

REFERENCES

[1] J. Böcker, “Tolerance band controller for a three-level four-quadrant converter including DC link balancing”, PESC Conference, Aachen, 2004.

[2] J. Böcker, “Discrete-Event Converter Control”, European Conf. on Power Electronics and Applications, Toulouse, 2003.

[3] J. W. Dixon, I. A. Leal, Current Control Strategy for Brushless DC Motors Based on a Common DC Signal”, IEEE Trans. Power Electronics, Vol. 17, No. 2, March 2002, pp.232-240

[4] A. Murray, P. Kettle, F. Moynihan, “Advances in Brushless DC Motors”, American Control Conference, 1997, Vol. 6, pp 3985-3989

[5] T. J. E. Miller, “Brushless Permanent Magnet and Reluctance Motor Drives”, Oxford Science Publications, 1993

[6] P. Muir, C.P. Neuman; “Pulsewidth Modulation Control of Brushless DC Motors for Robotic Applications”, IEEE Trans. Industrial Electronics, Vol. 32, No. 3, August, 1985, pp. 222-229.